THE JOURNAL OF PHYSICAL CHEMISTRY B

pubs.acs.org/JPCB Article

Direct Visualization of the Binding of Transforming Growth Factor Beta 1 with Cartilage Oligomeric Matrix Protein via High-Resolution Atomic Force Microscopy

Victoria Tran, Arpad Karsai, Michael C. Fong, Weiliang Cai, J. Gabriel Fraley, Jasper H.N. Yik, Eric Klineberg, Dominik R. Haudenschild, and Gang-yu Liu*

Cite This: J. Phys. Chem. B 2020, 124, 9497−9504

ABSTRACT: This work reports the first direct observations of binding and complex formation between transforming growth factor beta 1 (TGF-β1) and cartilage oligomeric matrix protein (COMP) using high-resolution atomic force microscopy (AFM). Each COMP molecule consists of pentamers whose five identical monomeric units bundle at N-termini. From this central point, the five monomers' flexible arms extend outward with C-terminal domains at the distal ends, forming a bouquet-like structure. In commonly used buffer solutions, TGF-β1 molecules typically form homodimers (majority), double dimers (minority), and aggregates (trace amount). Mixing TGF-β1 and COMP leads to rapid binding and complex formation. The TGF-β1/COMP complexes contain one to three COMP and multiple TGF-β1 molecules. For complexes with one COMP, the structure is more compact and less flexible than that of COMP alone. For complexes with two or more COMP molecules, the conformation varies to a large degree from one complex to another. This is attributed to the presence of double dimers or aggregates of TGF-β1 molecules, whose size and multiple binding sites enable binding to more than one COMP. The number and location of individual TGF-β1 dimers are also clearly visible in all complexes. This molecular-level information provides a new insight into the mechanism of chondrogenesis enhancement by TGF-β1/COMP complexes, i.e., simultaneous and multivalent presentation of growth factors. These presentations help explain the high efficacy in sustained activation of the signaling pathway to augment chondrogenesis.

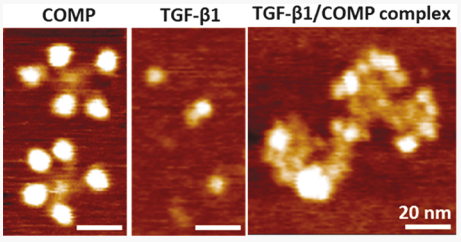

1. INTRODUCTION

Transforming growth factor beta 1 (TGF-β1) belongs to a superfamily of multifunctional growth factors that regulate a variety of biological functions, including cell proliferation, differentiation, and maturation.[1,2] It has been implicated as an important regulatory molecule during differentiation of mesenchymal stem cells (MSC) into chondrocytes for cartilage formation.[1] Recent studies have suggested that the manner in which growth factors are presented to cell surface receptors is vital for regulating and enhancing differentiation.[3,4] Prior investigation by our team discovered that the mixtures of TGF-β1 with cartilage oligomeric matrix protein (COMP), an extracellular matrix component, elicited a greater enhancement on the signaling transduction activity than TGF-β1 alone.[5] COMP (524 kDa) is a disulfide-bonded homopentameric glycoprotein found in the extracellular matrix of cartilage, tendons, bone tissues, and ligaments.[6,7] Its structure is composed of five identical monomers, each consisting of an N-terminal coiled-coil domain, four epidermal growth factor (EGF) repeats, eight thrombospondin-3 repeats, and a C-terminal domain.[8,9] The pentameric structure of COMP allows its simultaneous interaction with multiple entities, such as growth factors,[4,5,10] fibronectin,[11] and collagen.[12] Thus, COMP is recognized as a potential scaffold to coordinate the presentation of multiple growth factors to cells. For example, it was postulated that COMP and TGF-β1 formed complexes, and as such, enabled the multivalent presentation of growth factors and enhanced chondrogenesis.[5] However, the precise molecular interaction is not completely understood, such as the occupancy of growth factor binding sites on COMP. Hence, it is important to acquire molecular-level knowledge of the binding and conformation of each growth factor molecule in the complex, as the growth factor presentation directly impacts its subsequent interactions with cells, and the cellular signaling processes downstream.

Prior attempts to image these complexes included a negative stained transmission electron micrograph using colloidal a thiocyanate gold nanoparticle labeled TGF-β1 in conjunction

Received: August 9, 2020
Revised: September 24, 2020
Published: October 14, 2020

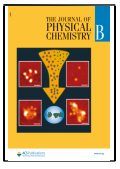

https://dx.doi.org/10.1021/acs.jpcb.0c07286
J. Phys. Chem. B 2020, 124, 9497−9504

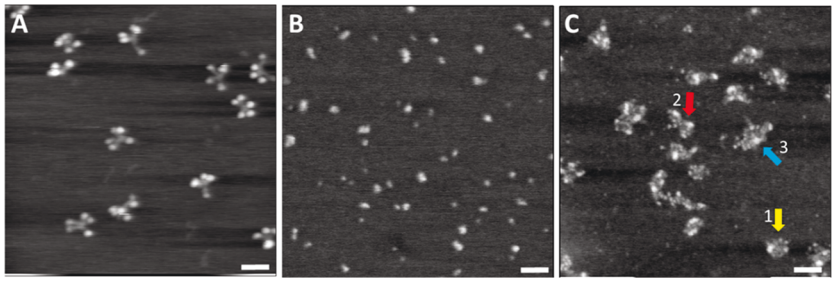

Figure 1. AFM topographic images of protein molecules immobilized on mica(0001) surfaces: (A) COMP molecules, (B) TGF-β1 molecules, and (C) a TGF-β1 and COMP mixture. TGF-β1/COMP complexes adopt geometries, such as "sea otter paw" (arrow 1), "butterfly" (arrow 2), and "stingray" (arrow 3). Tapping mode was used for image acquisition under a speed of 3.5 μm/s and 1024 × 512 pixels per frame. The scale bar is 50 nm, and the height contrast ranges 0−2.4 nm.

with protein fixation and uranyl formate stains.[5] However, the impact of labels and treatments on the reactivities and structural integrity remains unknown. Therefore, a label-free technology with the capability of imaging protein in buffer media is needed. Atomic force microscopy (AFM), known for being label-free, high-resolution, and versatile, provides a powerful tool to fill the void. In fact, AFM has been utilized to image a variety of biological specimens, including cells, proteins, and DNA at nanometer resolution.[13−20] AFM enables protein molecules to be visualized in buffer with nanometer resolution in three dimensions.[21−26] In fact, our prior work has demonstrated that AFM enabled high-resolution imaging of BMP-2/COMP complexes.[4] This work utilizes AFM to investigate the COMP and TGF-β1 systems to reveal the binding and structure of the complexes. The measured outcomes include direct observation of the proteins, and protein complex formation including TGF-β1 molecules within each complex. These observations provide a molecular level insight into the growth factor binding behavior and the mechanism for their enhancement of chondrogenesis.

2. EXPERIMENTAL SECTION

2.1. Materials Used for This Investigation. HEPES (1 M), hydrochloric acid (36.5−38.0% w/w), and TRIS (base) were ordered from Fisher Scientific (Hampton, NH). Phosphate-buffered saline (PBS) (1X) was purchased from Mediatech (Manassas, VA). Sodium chloride, NaCl (≥99%) and calcium chloride, $CaCl_2$ (≥96%) were all purchased from Sigma−Aldrich (St. Louis, MO). Deionized water with a resistivity of 18.2 MΩ·cm was generated using a Millipore Milli-Q system (EMD Millipore, Billerica, MA). Mica sheets were purchased from S & J Trading Inc. (Glen Oaks, NY). An Amicon centrifugal filter unit with 100 kDa molecular weight cutoff (catalog #: UFC910024) was purchased from Millipore Sigma (Burlington, MA).

2.2. Recombinant Human COMP and TGF-β1. Recombinant human COMP was expressed and purified as described previously.[5] Briefly, the COMP expression cassette was cloned into a pCCL3 lentiviral vector and transfected into human 293T cells (American Type Culture Collection, Manassas, VA) in a serum-free culture medium. The recombinant human COMP was purified from the cell culture medium to near homogeneity via nickel-NTA column affinity chromatography. After purification, the buffer exchange was done using the Amicon centrifugal filter unit with 100 kDa molecular weight cutoff, and the sample was concentrated to the desired concentration, typically 860 nM, using the same filter unit. Purified COMP was stored in a 20 mM HEPES buffer (pH 7.0), 500 mM NaCl, and 2 mM $CaCl_2$ at 4 °C.[27] Human TGF-β1 was purchased from PeproTech (Rocky Hill, NJ). Solid, white powder TGF-β1 was resuspended in 4 mM HCl to obtain a stock concentration of 7700 nM.

2.3. Protein Immobilization on Mica(0001) Surfaces. Protein immobilization followed our prior protocol.[4] The stock solution of COMP (860 nM) was diluted with 20 mM HEPES buffer (pH 6.8), 100 mM NaCl, and 2 mM $CaCl_2$ to a working concentration of 2 nM. A volume of 100 μL of the protein solution was deposited onto a freshly cleaved mica(0001) surface. After 2 min of absorption, the mica surface was washed with ultrapure Milli-Q water (18.2 MΩ cm) to remove loosely attached proteins and buffer residues. The samples were dried by gently blowing clean compressed air onto mica surfaces before AFM imaging. Immobilization of TGF-β1 followed the same protocols. The stock solution of TGF-β1 (7700 nM) was diluted with 20 mM HEPES buffer (pH 6.8), 100 mM NaCl, and 2 mM $CaCl_2$ to reach a working concentration of 20 nM.

The TGF-β1/COMP complex was formed by premixing COMP and TGF-β1 for 1 h at room temperature in 20 mM HEPES buffer (pH 6.8), 100 mM NaCl, and 2 mM $CaCl_2$ before deposition. The concentration of COMP and TGF in the solution was 2 nM and 20 nM, respectively. The pH of the binding buffers was set at 6.8 to ensure optimal binding of TGF-β1 to COMP.[5] Following the same procedures of protein deposition as described above, the protein complexes were immobilized onto freshly cleaved mica(0001) surfaces, washed with ultrapure water, and dried with compressed air. Samples were imaged immediately after drying.

For the concentration-dependent experiment, COMP and TGF-β1 were mixed in 50 mM Tris-buffered saline (TBS), pH 6.8, 150 mM NaCl and 16 mM $CaCl_2$. The concentration of TGF-β1 varied from 2−40 nM while maintaining the concentration of the COMP constant at 2 nM. A similar protocol as above was applied for immobilization of the mixture on the mica(0001) surface.

2.4. Atomic Force Microscopy. Atomic force microscopy (AFM) images were acquired using a commercial instrument (MFP-3D, Oxford Instruments, Santa Barbara, CA). The tapping mode and soft cantilevers were utilized to minimize perturbation to the immobilized protein molecules on surfaces.[13,16] All images were taken using an MSNL-10 cantilevers (Bruker Nano, Camarillo, CA) with a force constant of 0.6 N/m and a resonant frequency of 109 kHz. For tapping mode imaging under ambient conditions, the driving frequency, drive amplitude, and damping were set at 109 kHz, 0.30 V, and 25%, respectively. Data acquisition was

https://dx.doi.org/10.1021/acs.jpcb.0c07286
J. Phys. Chem. B 2020, 124, 9497−9504

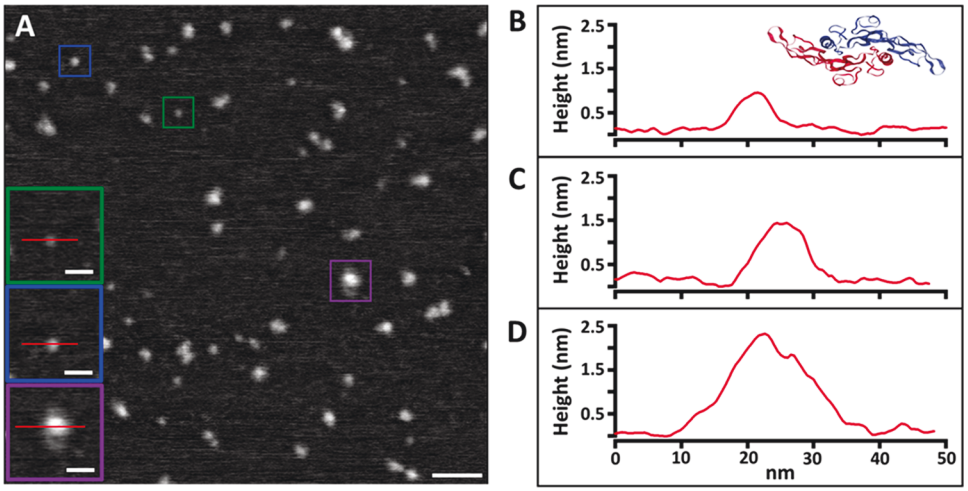

Figure 2. (A) AFM topographic images of immobilized TGF-β1 molecules on a mica(0001) surface. The scale bar is 50 nm. Insets are the zoom in views of three characteristic TGF-β1 features as indicated by the green, blue, and purple frames, respectively. Inset scale bar = 20 nm. (B−D) Cursor profiles as indicated in the green, blue, and purple insets, respectively. A TGF- β1 homodimer is displayed within the frame of (B) based on the known crystal structure (10.2210/pdb1KLD/pdb).

carried out using MFP-3D software developed based on the Igor Pro 6.12 platform.

3. RESULTS

3.1. High-Resolution AFM Images Reveal the Formation of the TGF-β1/COMP Complexes upon Mixing. We investigated the interaction of TGF-β1 and COMP by comparing high-resolution AFM images of the COMP, TGF-β1, and their mixtures after immobilization onto mica(0001) surfaces. Mica(0001) surfaces were chosen as the support because they are atomically flat structures.[4,22,28,29] In Figure 1, the characteristic AFM topographical images for all three systems are displayed side-by-side, using the same scanning size of 500 × 500 nm^2.

In Figure 1A, 100 μL of the 2 nM COMP solution was deposited onto mica(0001) for 2 min, followed by washing with Milli-Q water and drying with compressed air before AFM imaging. Individual COMP molecules were clearly separated and visualized. Each COMP adopts its individual conformation that can be described as a "gecko's foot". This morphology is a characteristic of a viable COMP molecule in buffer, as reported in our prior studies.[4] The globular end of each gecko finger appears brighter, i.e., taller than the arm, corresponding to the C-terminal domain. The orientation of each monomer within the pentameric COMP is also clearly visualized under AFM imaging. Consistent with prior reports, COMP molecules exist as a homopentameric glycoprotein composed of five identical units assembling together with N-termini at the center and C-termini at the distal end.[4,30−32] Molecules exhibited various conformations upon immobilization owing to the flexibility of its monomer arms and assembly.[4,5,30] The AFM morphology of COMP molecules is also consistent with prior X-ray crystallography of two truncated COMP and prior TEM studies of pentameric COMP, in which the N-termini of pentameric COMP bundles at the center, while the C-terminus extends outward.[5,9,27,32]

In Figure 1B, 100 μL of 20 nM TGF-β1 solution was pipetted onto mica(0001) for 2 min and then washed and dried prior to AFM imaging. Each bright bump corresponds to TGF-β1 molecules. It is known that TGF-β1 molecules exist as homodimers,[33,34] thus one would anticipate uniformly sized features in AFM topography. However, Figure 1B reveals variation of the feature size; therefore, we suspected that TGF-β1 under these conditions might have formed aggregates. The aggregation status has been analyzed in detail under higher resolution imaging as discussed in the next section.

Upon mixing TGF-β1 and COMP for 1 h, the mixture of TGF-β1 and COMP was then deposited onto mica(0001) following the same protocol as that in Figure 1A,B. The outcome, shown in Figure 1C, clearly reveals new features whose morphology significantly differs from either that of COMP or TGF-β1 alone. This is a direct and clear indication that binding occurred and TGF-β1/COMP complexes formed. From the size and overall morphology, the features can be categorized into two groups: (a) complexes containing one COMP molecule and multiple TGF-β1 molecules (e.g., arrow 1) and (b) complexes containing two or more COMP molecules and multiple TGF-β1 molecules (e.g., arrows 2 and 3). The complexes containing one COMP adopt a geometry that can be described as a "sea otter paw" (arrow 1). The complexes containing two COMP molecules adopt various conformations, e.g., the geometries of a "butterfly" (arrow 2) and a "stingray" (arrow 3). This finding is rational as the variation in molecular conformation increases with its size and complexity.

3.2. High-Resolution AFM Images Reveal Aggregation Status of TGF-β1 Molecules. Figure 2A shows TGF-β1 molecules from an aqueous solution containing 20 mM HEPES buffer (pH 6.8), 100 mM NaCl, and 2 mM $CaCl_2$. Under this condition, the TGF-β1 molecules have a positive net charge of +8, which was determined using the Prot pi calculator.[35] Upon immobilization onto a mica(0001) surface, AFM imaging were acquired using the tapping mode. The bright features in Figure 2A are attributed to TGF-β1 molecules. These features are well separated, yet vary in size, and thus are likely the results of various aggregations of TGF-β1 molecules in the solution. As TGF-β1 and bone morphogenetic protein-2 (BMP-2) are from the same TGF-β superfamily, we expect that the dimer form of these proteins would be comparable. The smallest features of TGF-β1 molecules, as shown in the green inset example, measures 6.4 nm wide, 7.5 nm long, and 1.0 nm tall (cursor, Figure 2B).

https://dx.doi.org/10.1021/acs.jpcb.0c07286
J. Phys. Chem. B 2020, 124, 9497−9504

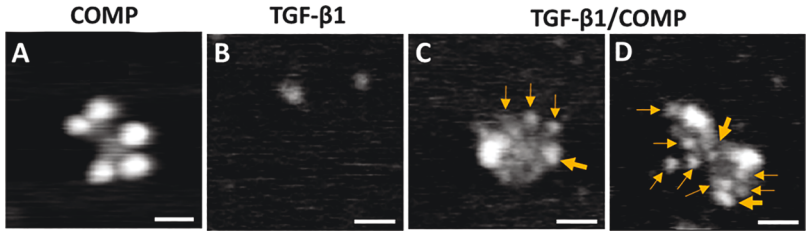

Figure 3. High-resolution AFM topographic images of representative protein molecules in this investigation: (A) COMP, (B) a TGF-β1 dimer and a double dimer, (C) a TGF-β1/COMP complex containing one COMP, and (D) a TGF-β1/COMP complex containing two COMP molecules. Yellow arrows point to TGF-β1 molecules within the complex; thin arrows indicate dimeric TGF-β1, and thick arrows indicate the double dimer TGF-β1. Scale bars = 20 nm.

These measurements are similar to that of BMP-2 dimers (7.5 ± 1.3 nm wide, 10.0 ± 2.0 nm long, and 0.8 ± 0.1 nm tall) under AFM imaging in ambient conditions. Therefore, these smallest features are consistent with TGF-β1 dimers immobilized with the molecular axis parallel to the mica surface, i.e., belly down, as illustrated via the protein model in Figure 2B. TGF-β1 dimers represents 41% of the protein population in the solution. The next size up, e.g., in the blue inset, measures 10.3 nm wide, 11.7 nm long, and 1.3 nm tall (cursor, Figure 2C), almost twice in volume as that of the TGF-β1 dimers, which are consistent with a double dimer. The double dimer represents 16% of the TGF-β1 population. Large aggregates are also present, for example, the purple inset measures 12.9 nm × 14.5 nm × 2.3 nm (cursor, Figure 2D). These aggregates make up 23% of the protein populations. The other 20% of the TGF-β1 population are between the double dimer and aggregate of dimers in size. In contrast to BMP-2 solutions, which contain nearly 100% dimers,[4] TGF-β1 molecules in solution exhibit dimers, double dimers, aggregations, i.e., heterogeneity in aggregation status in standard buffer solutions (20 mM HEPES buffer at pH 6.8, 100 mM NaCl, and 2 mM $CaCl_2$). These observations were reproducible among all five independent experiments, each imaged with multiple randomly selected areas. As will be discussed in detail in later sections, the aggregation leads to complexity and rich structures in TGF-β1/COMP binding.

3.3. High-Resolution AFM Images Reveal Structural Details within the TGF-β1/COMP Complexes. While we concluded from Figure 1 that binding occurred when mixing TGF-β1 and COMP, additional structural information requires a zoom in view of protein molecules. Figure 3 shows representative high-resolution images of the protein systems under this investigation. Figure 3A displays the characteristic pentameric structure of COMP molecules to which the complex images will be compared to reveal binding information. Immobilized COMP molecules were also imaged in buffer solutions. The morphology and apparent height measurements are very similar to that shown in Figures 1A and 3A. A TGF-β1 dimer and a double dimer are displayed in Figure 3B, whose dimensions provide a guide to identify the location of TGF-β1 molecules in the TGF-β1/COMP complexes.

Figure 3C shows a TGF-β1/COMP complex containing one COMP molecule. This complex exhibits geometry like that of a sea otter paw, with 5 toes at the top of the periphery. Four out of the five toe-like features are assigned as the TGF-β1 molecules (arrows). Key evidence arises from the disappearance of the C-terminal domains of the COMP in those arms and the comparison of topographic dimensions with that in Figure 3B. The C-terminal domains of the COMP undergo a conformational change to bind growth factor molecules.[4] The bright domain on the right is likely due to the remaining arm of the COMP not reacting with TGF-β1. In this complex, 3 out of 5 arms of the COMP are bound to three TGF-β1 dimers (thin arrows), respectively, and one arm (right) is bound to a TGF-β1 double dimer (thick arrow). Comparing Figure 3A with Figure 3C, it is evident that the TGF-β1/COMP complex exhibits a more compact structure than that of a COMP molecule: monomer arms of the COMP are well spread, while arms of the TGF-β1/COMP are hardly recognizable. The compactness can be estimated quantitatively from the AFM topography by taking the ratio of the occupied area over the total footprint area: 68% for the COMP shown in Figure 3A versus 98% in Figure 3C. The compactness of the complex could explain its lower flexibility than that of COMP.[4]

Figure 3D shows another TGF-β1/COMP complex, whose geometry resembles that of a butterfly. The footprint of this complex is almost 1.5 times as large as that in Figure 3C, thus we infer that two COMP molecules participated in the reaction. Nine TGF-β1 binding sites scattered within the complex can be clearly visualized, as indicated by arrows. Comparing its size with that in Figure 3B, these sites consist of seven TGF-β1 dimers (arrows) and one double dimer (thicker arrow at the lower right). The two bright features atop of the two butterfly wings are consistent with the C-terminal domains in COMP, thus are assigned to the unbound sites. This complex is also more compact than that of COMPs, estimated to be 77% in comparison to the 68% of the COMP. Although appearing small, the TGF-β1 site in the middle of the butterfly joining the two COMPs is likely a double dimer, whose location and orientation are so well inlaid that only a small portion is visible under AFM. The binding sites in each TGF-β1 double dimer are twice as many as that in a dimer. The longest binding site separation in the double dimer is also larger than that in a single dimer. Therefore, the chance for a double dimer to capture two COMP molecules is enhanced. In addition to the sea otter paw and butterfly conformation, other conformations of the TGF-β1/COMP complex are also captured faithfully by AFM, e.g., a stingray as indicted by arrow three in Figure 1C. Because of the size and complexity of the complexes containing two COMPs, conformations vary to a larger degree than complexes containing a single COMP. These observations were reproducible in all five independent experiments, each imaged with multiple randomly selected areas.

3.4. Structure and Conformation of TGF-β1/COMP Complexes Vary with the Increase of TGF-β1 Concentration. Using the same COMP concentration (2 nM) as the experiment shown in Figure 1, we increased the concentration of TGF-β1 from 2 to 40 nM, and as such, the molar ratio of

https://dx.doi.org/10.1021/acs.jpcb.0c07286
J. Phys. Chem. B 2020, 124, 9497−9504

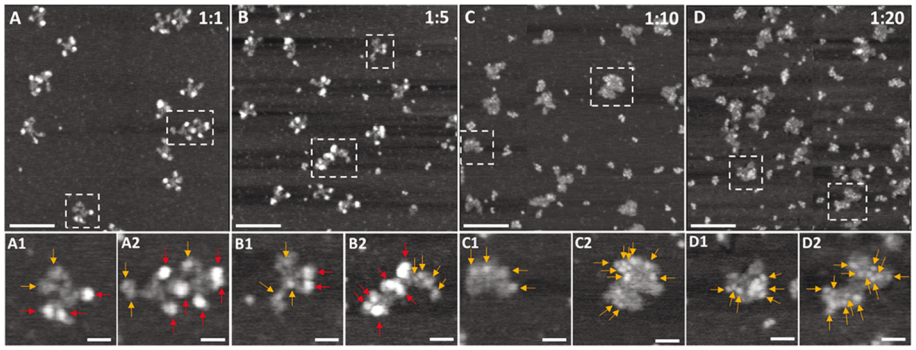

Figure 4. Top row: AFM topographic images of immobilized TGF-β1 and COMP mixtures at the designed COMP:TGF-β1 ratio as indicated at the top right of each frame. Scale bar = 100 nm. Bottom row: Zoom in views of two representative complexes selected from the frame above, containing one and two COMP molecules, respectively. Red arrows indicate C-terminal domains of COMP, and yellow arrows point to the location of the TGF-β1 molecules in the complexes. Scale bar = 20 nm.

COMP:TGF-β1 decreased from 1:1 to 1:20. Figure 4 compares the trend of the formation of the complex with the decrease of the COMP:TGF-β1 ratio.

The effects of the molar ratio of COMP:TGF-β1 on unbound TGF-β1 molecules were clearly seen when comparing Figure 4A–D. Two trends were observed: the number of unbound TGF-β1 molecules increased with the increase of the TGF-β1 concentration or the decrease of the COMP:TGF-β1 ratio, and more and more unbound double dimers and aggregates appeared as well. Focusing on the areas without the complexes: at a ratio of 1:1, two TGF-β1 dimer molecules were clearly visible in Figure 4A. When the ratio was decreased to 1:5 (Figure 4B), there were almost 6 times unbound and free TGF-β1 dimers as that in Figure 4A. Not only were TGF-β1 dimers present but also 14 small clustering of TGF-β1 dimers, e.g., double dimers and aggregates, were seen. At the ratio of 1:10, six individual TGF-β1 dimers, and 22 TGF-β1 double dimers and aggregates were observed in Figure 4C. The amount of unbound TGF-β1 double dimers and aggregates doubled in comparison to Figure 4B. The trends continue; in Figure 4D at the 1:20 ratio, there were 12 TGF-β1 dimers and 36 double dimers and aggregates, respectively.

Three trends regarding the TGF-β1/COMP complexes were clearly observed comparing all images in Figure 4 from left to right. First, the population of complexes containing two COMPs increased approximately 2 times the amount as the COMP:TGF-β1 ratio decreased to 1:20. For each sample, at least eight images were acquired, from which we counted the number of complexes containing two COMPs versus the total populations. At a 1:1 ratio (e.g., Figure 4A), the majority of the population of the complex contains one COMP, and only 13% $\pm$ 3% of the population contained two COMPs, which was taken from eight number of images in this investigation. At a ratio of 1:5 (e.g., Figure 4B), the complex population containing two COMPs reaches 15% $\pm$ 5%. At a ratio of 1:10 (e.g., Figure 4C), 10% $\pm$ 5% of the population contained two COMPs. Decreasing the ratio to 1:20 (e.g., Figure 4D), 23% $\pm$ 5% complexes had two COMPs, which is approximately 2 times as that in Figure 4A. Though the population of complexes containing two COMPs does not increase with the ratio of COMP:TGF-β1, it is evident that the formation of two COMP complexes increase with more TGF-β1.

Second, comparing complexes containing one COMP, the number of TGF-β1 molecules per complex increased with the increasing TGF-β1 concentration. In Figure 4A1 with the COMP:TGF-β1 ratio of 1:1, two TGF-β1 molecules were clearly seen (yellow arrows), while the other three monomer units in COMP did not participate in binding, as characterized by the bright C-terminal domains (red arrows). The apparent height of these C-termini measured as 1.9 $\pm$ 0.2 nm is consistent with the known AFM topography of COMP.[4] Decreasing the ratio to 1:5, Figure 4B1 shows that three TGF-β1 molecules bound to COMP and only two unbound arms remained. At the ratio of 1:10, the characteristic gecko's foot conformation of the COMP completely vanished, and the complex exhibited a more compact conformation of sea otter paw, as shown in Figure 4C1. Four TGF-β1 molecules are clearly visible, but we infer five binding events from the lack of C-terminal domains in Figure 4C1. At a ratio of 1:20, at least six TGF-β1 molecules could be clearly identified in the complex shown in Figure 4D1, which is more than the conventional view of five binding sites per COMP. The presence of TGF-β1 double dimers and aggregates is attributed to the observations of >5 TGF-β1 dimers/COMP.

Third, for complexes containing two COMP molecules, the number of TGF-β1 molecules per complex increased with the decreasing COMP:TGF-β1 ratio. We note that not all TGF-β1 dimers could be captured in those cases due to the complexity in the conformation and binding location, e.g., growth factors were only partly exposed or completely hidden from outmost surfaces. Therefore, the TGF-β1 dimers identified from AFM images represent the minimum number of binding events. At the 1:1 ratio, shown in Figure 4A2, at least three TGF-β1 molecules were visible (yellow arrows), while six monomers in the COMP remain unbound (red arrows). At the 1:5 ratio, the complex in Figure 4B2 contained at least four TGF-β1 dimers. The number of TGF-β1 binding event increased to 10 in Figure 4C2, at the ratio of 1:10. At the ratio COMP:TGF-β1 = 1:20, the number of TGF-β1 per complex increased further, as shown in Figure 4D2, where at least 13 TGF-β1 dimers were clearly visualized. These observations demonstrate the robustness of our conclusion that TGF-β1/COMP complexes formed upon mixing and suggest that double dimers and aggregates of TGF-β1 were responsible for the formation of large complexes (i.e., more than one COMP) and large numbers of TGF-β1 dimers in these complexes.

4. DISCUSSION

It is known that each COMP molecule has five high-affinity binding sites for growth factors such as TGF-β1 and BMP-2.[5,6,10] Prior studies have shown that binding likely occurs in

https://dx.doi.org/10.1021/acs.jpcb.0c07286
J. Phys. Chem. B 2020, 124, 9497–9504

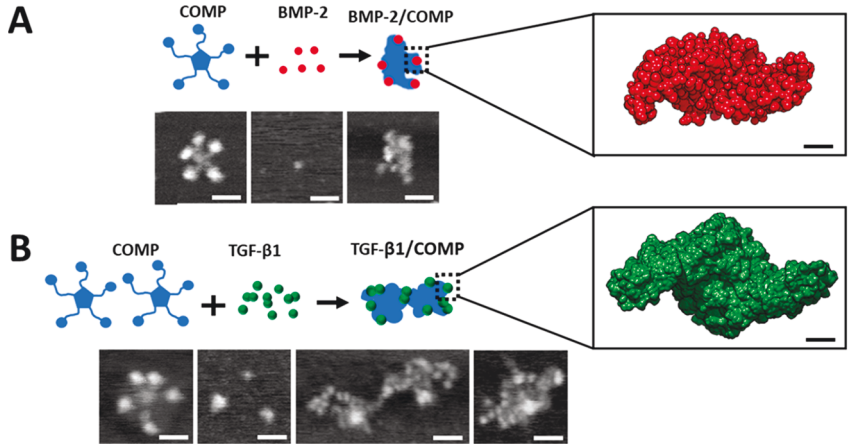

Figure 5. (A) Schematic diagram of BMP-2 binding with COMP. Corresponding AFM images are shown below. Scale bar among AFM images = 25 nm. (B) Schematic diagram of TGF-β1 binding with COMP. Scale bar among AFM images = 25 nm. The volume filing models of BMP-2 (10.2210/pdb3BMP/pdb) and TGF-β1 (10.2210/pdb1KLA/pdb) are compared. The 3D size of a BMP-2 and TGF-β1 dimer is ~7.0 nm × 3.5 nm × 3.0 nm and ~ 9.0 nm × 4.0 nm × 3.0 nm, respectively. Scale bar among protein models = 1 nm.

the C-terminal region (~200 residues) using hybrid β-galactosidase and in vitro GST pull-down assays.[27,36] TGF-β1 and BMP-2 belong to the transforming growth factor superfamily and likely bind to the general C-terminal region of COMP.[5,6,37,38] In fact, our past and current investigations revealed similarities among TGF-β1/COMP and BMP-2/COMP binding: (a) C-terminal domains of COMP, which are typically taller than the chain due to folded conformation undergo a conformation change due to binding of growth factors, and (b) the complexes are more densely packed and less flexible than COMP, as illustrated in Figure 5. We describe COMP geometry as a gecko's foot, which is flexible and spread out. By comparison, TGF-β1/COMP and BMP-2/COMP complexes resemble to a "sea otter paw" and "gummy bear", respectively.

Figure 5 also illustrates key differences between TGF-β1 and BMP-2 in the context of their binding with COMP. Almost all BMP-2/COMP complexes contain only one COMP per complex, exhibiting various gummy bear morphologies under AFM imaging, as shown in Figure 5A. In contrast, the majority of TGF-β1/COMP complexes contain one COMP per complex, but some TGF-β1/COMP complexes contain two or more COMPs, as illustrated in Figure 5B. These large complexes exhibit a wider range of conformations, e.g., butterfly or stingray. As illustrated in Figure 5B, the formation of these large complexes is attributed to the double dimers or aggregates of TGF-β1 molecules, whose size and multiple binding sites enable binding to more than one COMP.

Another difference arises from the observation that TGF-β1 molecules in the complexes appear taller and more clearly resolved than that of BMP-2 molecules. We attribute this observation to the differences in molecular dimension and their binding behavior to COMP. The geometry and dimensions of TGF-β1 and BMP-2 dimers can be found from the PDB and are compared in Figure 5.[38,39] Clearly, TGF-β1 is physically larger than BMP-2, thus more visible in AFM topographic images. In addition, BMP-2 dimers are likely more inlaid in the binding pockets of the COMP than those of TGF-β1 dimers, i.e., the presentation of TGF-β1 is more exposed.

While TGF-β1 and BMP-2 belong in the same TGF superfamily and have a relatively similar structure, they exhibit characteristic differences in their binding interactions with their respective receptors.[6,38] TGF-β1 binds only to Type I (TβR-I) and Type II (TβR-II) receptors, while BMP-2 can interact with two Type I (Alk1, Alk2) and three Type II (ActR-II, ActR-IIb and BMPR-II) receptors.[38] Our observed differences of BMP-2 and TGF-β1 binding behavior to COMP also help rationalizing their different interactions with these receptors. Prior investigations by our team reported that the mixtures of TGF-β1 with COMP elicited a greater enhancement on the signalling transduction activity than TGF-β1 alone.[5] We infer that the presentation of TGF-β1 molecules in the TGF-β1/COMP complexes expose the binding domains to receptors and allow simultaneous and multivalent binding to receptors. The multivalent presentations lead to high efficacy in the sustained activation of the signaling pathway to augment chondrogenesis. Other signaling processes could also be impacted by the presentation of growth factors. Recent studies have suggested that the manner in which growth factors are presented to the cell receptors is vital for regulating and enhancing differentiation.[3]

5. CONCLUSIONS

This work presents the first direct observations of binding and complex formation between TGF-β1 and COMP molecules using high-resolution AFM imaging. Exploiting the high spatial resolution and label-free nature of AFM, this investigation indicated that TGF-β1 molecules exhibit as homodimers (majority), double dimers, and aggregates in commonly used buffers (e.g., pH = 6.8 and 20 mM HEPES buffer with 100 mM NaCl and 2 mM $CaCl_2$). Individual COMP molecules adopt a pentameric structure whose five identical monomer units bundle at N-termini. From this central point, the five flexible monomer chains extend to C-terminal domains at the distal ends, whose conformations are bulkier than the chains. Mixing COMP and TGF-β1 in buffer led to formation of complexes quickly in room temperature. The TGF-β1/COMP complexes contain one to three COMP and multiple TGF-β1 dimers. For complexes with one COMP, the structure is more compact and less flexible than that of the COMP alone. For complexes with two or more COMP molecules, the conformation varies significantly from one complex to another. The formation of these large complexes is attributed to the double dimers or

https://dx.doi.org/10.1021/acs.jpcb.0c07286
J. Phys. Chem. B 2020, 124, 9497−9504

aggregates of TGF-β1 molecules, whose sizes and multiple binding sites enable binding to more than one COMP. The formation of large complexes occurred more frequently in the case of TGF-β1 and COMP binding, in contrast to that of BMP-2 and COMP. The number and location of individual TGF-β1 dimers are also clearly visible in the TGF-β1/COMP complexes. In most cases, 1−5 TGF-β1 dimers per COMP were seen among complexes, consistent with the knowledge that each COMP contains five strong binding sites to growth factors. In some cases, more than five TGF-β1 dimers per COMP were seen. The formation of large complexes and binding with more than five TGF-β1 dimers per COMP represent another key difference from that of BMP-2/COMP complexes. This molecular-level information provides new insights into the mechanism of chondrogenesis enhancement by TGF-β1/COMP complexes, i.e., simultaneous and multivalent presentation of growth factors. Revealing the multivalent presentation of TGF-β1 molecules deepens our understanding of the high efficacy in sustained activation of the signaling pathway to augment chondrogenesis.

AUTHOR INFORMATION

Corresponding Author

Gang-yu Liu − *Department of Chemistry, University of California, Davis, California 95616, United States*; Phone: (530) 754-9678; Email: gyliu@ucdavis.edu; Fax: (530) 754-8557

Authors

Victoria Tran − *Department of Chemistry, University of California, Davis, California 95616, United States*

Arpad Karsai − *Department of Chemistry, University of California, Davis, California 95616, United States*

Michael C. Fong − *Department of Biomedical Engineering, University of California, Davis, California 95616, United States*

Weiliang Cai − *Department of Orthopaedic Surgery, University of California-Davis Medical Center, Sacramento, California 95817, United States*

J. Gabriel Fraley − *Department of Orthopaedic Surgery, University of California-Davis Medical Center, Sacramento, California 95817, United States*

Jasper H.N. Yik − *Department of Orthopaedic Surgery, University of California-Davis Medical Center, Sacramento, California 95817, United States*

Eric Klineberg − *Department of Orthopaedic Surgery, University of California-Davis Medical Center, Sacramento, California 95817, United States*

Dominik R. Haudenschild − *Department of Orthopaedic Surgery, University of California-Davis Medical Center, Sacramento, California 95817, United States*

Complete contact information is available at: https://pubs.acs.org/10.1021/acs.jpcb.0c07286

Notes

The authors declare no competing financial interest.

ACKNOWLEDGMENTS

This work was supported by UC Davis, the National Institutes of Health (R01-AR070239), Department of Defense (CDMRP-PR142010), National Science Foundation (CHE-1808829), and the Gordon and Betty Moore Foundation.

REFERENCES

(1) Mizuta, H.; Sanyal, A.; Fukumoto, T.; Fitzsimmons, J. S.; Matsui, N.; Bolander, M. E.; Oursler, M. J.; O'Driscoll, S. W. The Spatiotemporal Expression of Tgf-β1 and Its Receptors During Periosteal Chondrogenesis in Vitro. *J. Orthop. Res.* **2002**, *20*, 562−574.

(2) Clark, D. A.; Coker, R. Transforming Growth Factor-Beta (Tgf-Beta). *Int. J. Biochem. Cell Biol.* **1998**, *30*, 293−298.

(3) Re'em, T.; Kaminer-Israeli, Y.; Ruvinov, E.; Cohen, S. Chondrogenesis of Hmsc in Affinity-Bound Tgf-β Scaffolds. *Biomaterials* **2012**, *33*, 751−761.

(4) Tran, V.; Karsai, A.; Fong, M. C.; Cai, W.; Yik, J. H. N.; Klineberg, E.; Haudenschild, D. R.; Liu, G.-Y. Label-Free and Direct Visualization of Multivalent Binding of Bone Morphogenetic Protein-2 with Cartilage Oligomeric Matrix Protein. *J. Phys. Chem. B* **2019**, *123*, 39−46.

(5) Haudenschild, D. R.; Hong, E.; Yik, J. H. N.; Chromy, B.; Mörgelin, M.; Snow, K. D.; Acharya, C.; Takada, Y.; Di Cesare, P. E. Enhanced Activity of Transforming Growth Factor Beta1 (Tgf-β1) Bound to Cartilage Oligomeric Matrix Protein. *J. Biol. Chem.* **2011**, *286*, 43250−43258.

(6) Acharya, C.; Yik, J. H. N.; Kishore, A.; Van Dinh, V.; Di Cesare, P. E.; Haudenschild, D. R. Cartilage Oligomeric Matrix Protein and Its Binding Partners in the Cartilage Extracellular Matrix: Interaction, Regulation and Role in Chondrogenesis. *Matrix Biol.* **2014**, *37*, 102−111.

(7) Hedbom, E.; Antonsson, P.; Hjerpe, A.; Aeschlimann, D.; Paulsson, M.; Rosa-Pimentel, E.; Sommarin, Y.; Wendel, M.; Oldberg, A.; Heinegård, D. Cartilage Matrix Proteins - an Acidic Oligomeric Protein (Comp) Detected Only in Cartilage. *J. Biol. Chem.* **1992**, *267*, 6132−6136.

(8) Efimov, V. P.; Engel, J.; Malashkevich, V. N. Crystallization and Preliminary Crystallographic Study of the Pentamerizing Domain from Cartilage Oligomeric Matrix Protein: A Five-Stranded α-Helical Bundle. *Proteins* **1996**, *24*, 259−262.

(9) Malashkevich, V. N.; Kammerer, R. A.; Efimov, V. P.; Schulthess, T.; Engel, J. The Crystal Structure of a Five-Stranded Coiled Coil in Comp: A Prototype Ion Channel? *Science* **1996**, *274*, 761−765.

(10) Ishida, K.; Acharya, C.; Christiansen, B. A.; Yik, J. H. N.; DiCesare, P. E.; Haudenschild, D. R. Cartilage Oligomeric Matrix Protein Enhances Osteogenesis by Directly Binding and Activating Bone Morphogenetic Protein-2. *Bone* **2013**, *55*, 23−35.

(11) Di Cesare, P. E.; Chen, F. S.; Moergelin, M.; Carlson, C. S.; Leslie, M. P.; Perris, R.; Fang, C. Matrix-Matrix Interaction of Cartilage Oligomeric Matrix Protein and Fibronectin. *Matrix Biol.* **2002**, *21*, 461−470.

(12) Blumbach, K.; Niehoff, A.; Paulsson, M.; Zaucke, F. Ablation of Collagen Ix and Comp Disrupts Epiphyseal Cartilage Architecture. *Matrix Biol.* **2008**, *27*, 306−318.

(13) Siedlecki, C. A.; Marchant, R. E. Atomic Force Microscopy for Characterization of the Biomaterial Interface. *Biomaterials* **1998**, *19*, 441−454.

(14) Dorn, I. T.; Eschrich, R.; Seemüller, E.; Guckenberger, R.; Tampé, R. High-Resolution Afm-Imaging and Mechanistic Analysis of the 20 S Proteasome. *J. Mol. Biol.* **1999**, *288*, 1027−1036.

(15) Hansma, H. G. Atomic Force Microscopy of Biomolecules. *J. Vac. Sci. Technol., B: Nanotechnol. Microelectron.: Mater., Process., Meas., Phenom.* **1996**, *14*, 1390−1394.

(16) Fotiadis, D.; Scheuring, S.; Müller, S. A.; Engel, A.; Müller, D. J. Imaging and Manipulation of Biological Structures with the Afm. *Micron* **2002**, *33*, 385−397.

(17) Hansma, H. G.; Sinsheimer, R. L.; Groppe, J.; Bruice, T. C.; Elings, V.; Gurley, G.; Bezanilla, M.; Mastrangelo, I. A.; Hough, P. V. C.; Hansma, P. K. Recent Advances in Atomic-Force Microscopy of DNA. *Scanning* **1993**, *15*, 296−299.

(18) Wadu-Mesthrige, K.; Amro, N. A.; Liu, G. Y. Immobilization of Proteins on Self-Assembled Monolayers. *Scanning* **2000**, *22*, 380−388.

(19) Liu, G. Y.; Amro, N. A. Positioning Protein Molecules on Surfaces: A Nanoengineering Approach to Supramolecular Chemistry. *Proc. Natl. Acad. Sci. U. S. A.* **2002**, *99*, 5165−5170.
(20) Tan, Y. H.; Liu, M.; Nolting, B.; Go, J. G.; Gervay-Hague, J.; Liu, G. Y. A Nanoengineering Approach for Investigation and Regulation of Protein Immobilization. *ACS Nano* **2008**, *2*, 2374−2384.
(21) Patil, S.; Martinez, N. F.; Lozano, J. R.; Garcia, R. Force Microscopy Imaging of Individual Protein Molecules with Sub-Pico Newton Force Sensitivity. *J. Mol. Recognit.* **2007**, *20*, 516−523.
(22) Viani, M. B.; Pietrasanta, L. I.; Thompson, J. B.; Chand, A.; Gebeshuber, I. C.; Kindt, J. H.; Richter, M.; Hansma, H. G.; Hansma, P. K. Probing Protein-Protein Interactions in Real Time. *Nat. Struct. Biol.* **2000**, *7*, 644−647.
(23) Bitler, A.; Lev, N.; Fridmann-Sirkis, Y.; Blank, L.; Cohen, S. R.; Shai, Y. Kinetics of Interaction of Hiv Fusion Protein (Gp41) with Lipid Membranes Studied by Real-Time Afm Imaging. *Ultramicroscopy* **2010**, *110*, 694−700.
(24) Wang, Z.; Zhou, C.; Wang, C.; Wan, L.; Fang, X.; Bai, C. Afm and Stm Study of Beta-Amyloid Aggregation on Graphite. *Ultramicroscopy* **2003**, *97*, 73−79.
(25) Valle, F.; DeRose, J. A.; Dietler, G.; Kawe, M.; Plückthun, A.; Semenza, G. Afm Structural Study of the Molecular Chaperone Groel and Its Two-Dimensional Crystals: An Ideal ″Living″ Calibration Sample. *Ultramicroscopy* **2002**, *93*, 83−89.
(26) Zykwinska, A.; Marquis, M.; Sinquin, C.; Marchand, L.; Colliec-Jouault, S.; Cuenot, S. Investigation of Interactions between the Marine Gy785 Exopolysaccharide and Transforming Growth Factor-β1 by Atomic Force Microscopy. *Carbohydr. Polym.* **2018**, *202*, 56−63.
(27) Tan, K.; Duquette, M.; Joachimiak, A.; Lawler, J. The Crystal Structure of the Signature Domain of Cartilage Oligomeric Matrix Protein: Implications for Collagen, Glycosaminoglycan and Integrin Binding. *Fed. Am. Soc. Exp. Biol. J.* **2009**, *23*, 2490−2501.
(28) Bergkvist, M.; Carlsson, J.; Karlsson, T.; Oscarsson, S. Tm-Afm Threshold Analysis of Macromolecular Orientation: A Study of the Orientation of Igg and Ige on Mica Surfaces. *J. Colloid Interface Sci.* **1998**, *206*, 475−481.
(29) Karsai, A.; Slack, T. J.; Malekan, H.; Khoury, F.; Lin, W. F.; Tran, V.; Cox, D.; Toney, M.; Chen, X.; Liu, G. Y. Local Mechanical Perturbation Provides an Effective Means to Regulate the Growth and Assembly of Functional Peptide Fibrils. *Small* **2016**, *12*, 6407−6415.
(30) DiCesare, P. E.; Mörgelin, M.; Carlson, C. S.; Pasumarti, S.; Paulsson, M. Cartilage Oligomeric Matrix Protein - Isolation and Characterization from Human Articular-Cartilage. *J. Orthop. Res.* **1995**, *13*, 422−428.
(31) Engel, J.; Furthmayr, H. Electron-Microscopy and Other Physical Methods for the Characterization of Extracellular-Matrix Components - Laminin, Fibronectin, Collagen-Iv, Collagen-Vi, and Proteoglycans. *Methods Enzymol.* **1987**, *145*, 3−78.
(32) Mörgelin, M.; Heinegard, D.; Engel, J.; Paulsson, M. Electron-Microscopy of Native Cartilage Oligomeric Matrix Protein Purified from the Swarm Rat Chondrosarcoma Reveals a 5-Armed Structure. *J. Biol. Chem.* **1992**, *267*, 6137−6141.
(33) Hinck, A. P.; Archer, S. J.; Qian, S. W.; Roberts, A. B.; Sporn, M. B.; Weatherbee, J. A.; Tsang, M. L. S.; Lucas, R.; Zhang, B. L.; Wenker, J.; et al. Transforming Growth Factor Beta 1: Three-Dimensional Structure in Solution and Comparison with the X-Ray Structure of Transforming Growth Factor Beta 2. *Biochemistry* **1996**, *35*, 8517−8534.
(34) Shi, M.; Zhu, J.; Wang, R.; Chen, X.; Mi, L.; Walz, T.; Springer, T. A. Latent Tgf-β Structure and Activation. *Nature* **2011**, *474*, 343−349.
(35) Josuran, R. *Prot Pi | Protein Tool*. https://www.protpi.ch/Calculator/ProteinTool (accessed September 16, 2020).
(36) Du, Y.; Wang, Y.; Wang, L.; Liu, B.; Tian, Q.; Liu, C. J.; Zhang, T.; Xu, Q.; Zhu, Y.; Ake, O.; et al. Cartilage Oligomeric Matrix Protein Inhibits Vascular Smooth Muscle Calcification by Interacting with Bone Morphogenetic Protein-2. *Circ. Res.* **2011**, *108*, 917−928.
(37) Gordon, K. J.; Blobe, G. C. Role of Transforming Growth Factor-Beta Superfamily Signaling Pathways in Human Disease. *Biochim. Biophys. Acta, Mol. Basis Dis.* **2008**, *1782*, 197−228.
(38) Hinck, A. P. Structural Studies of the Tgf-β S and Their Receptors - Insights into Evolution of the Tgf-β Superfamily. *Fed. Eur. Biochem. Soc., Lett.* **2012**, *586*, 1860−1870.
(39) Scheufler, C.; Sebald, W.; Hülsmeyer, M. Crystal Structure of Human Bone Morphogenetic Protein-2 at 2.7 Angstrom Resolution. *J. Mol. Biol.* **1999**, *287*, 103−115.

https://dx.doi.org/10.1021/acs.jpcb.0c07286
J. Phys. Chem. B 2020, 124, 9497−9504